Analysis and Multiple Steady States of an Industrial Heterogeneous Azeotropic Distillation

Marion Alliet, Vincent Gerbaud, Xavier Joulia, Pierre Sere Peyrigain, Michel Pons

▶ **To cite this version:**

Marion Alliet, Vincent Gerbaud, Xavier Joulia, Pierre Sere Peyrigain, Michel Pons. Analysis and Multiple Steady States of an Industrial Heterogeneous Azeotropic Distillation. Industrial & Engineering Chemistry Research, 2001, 4 (13), pp.2914-2924. 10.1021/ie000808s . hal-03483870

HAL Id: hal-03483870
https://hal.science/hal-03483870

Submitted on 16 Dec 2021

HAL is a multi-disciplinary open access archive for the deposit and dissemination of scientific research documents, whether they are published or not. The documents may come from teaching and research institutions in France or abroad, or from public or private research centers.

L'archive ouverte pluridisciplinaire **HAL**, est destinée au dépôt et à la diffusion de documents scientifiques de niveau recherche, publiés ou non, émanant des établissements d'enseignement et de recherche français ou étrangers, des laboratoires publics ou privés.

Analysis and Multiple Steady States of an Industrial Heterogeneous Azeotropic Distillation

Marion Alliet Gaubert,[†] Vincent Gerbaud,[*,†] Xavier Joulia,[†] Pierre Sere Peyrigain,[‡] and Michel Pons[§]

Laboratoire de Génie Chimique (LGC, UMR-CNRS 5503), INPT, ENSIACET, 18 Chemin de la Loge, F-31078 Toulouse Cedex 04, France, ProSim S.A., Route d'Espagne, F-31000 Toulouse, France, and Centre Technique de Lyon, ATOFINA, Chemin de la Lone, BP 32, F-36492 Pierre-Benite Cedex, France

A study of an industrial multicomponent heterogeneous azeotropic distillation is presented. The process concerns an organic acid dehydration using an immiscible entrainer. First, a validation of the MESH and thermodynamic models through a comparison between pilot-plant experimental reconciled data and simulation results is conducted. A four-component mixture is considered for the simulation. Case studies of the boiler heat duty are automatically generated by an operating path tool. An ∞/∞ analysis is performed for the heterogeneous azeotropic pilot column and an industrial column with a decanter. Because of practical constraints, the pilot and the industrial columns do not have the same reflux policies. This leads the ∞/∞ analysis to predict multiple steady states for the industrial unit but not for the pilot column. However, multiple steady states are found by simulation both for the pilot and for the industrial unit. Multiple steady states are confirmed by simulation and experimental data for the industrial unit. Because of the positive ∞/∞ analysis, they are attributed to the phase equilibrium properties of the quaternary system. For the pilot column, multiple steady states are found by the simulation and linked to experimental observations. The multiplicity is not caused by the phase equilibrium properties; rather, it is attributed to interactions between the material and energy balances. An analysis of the simulation results helps explain the behavior of the industrial unit: the temperature of the sensitive tray gives rise to a peak in heat. This peak is located very close to the industrial temperature set point and is correlated with an impurity content minimum in the main product stream. An impurity minimum is also evidenced by the simulation for the pilot column. This complex behavior can explain observed difficulties in controlling the process at the industrial set point.

1. Introduction

The separation by distillation of mixtures exhibiting azeotropes is a challenge as it is not possible to pass through the azeotropic limit by direct distillation. A common method of facilitating the separation is to add a chemical agent (called an entrainer or solvent) that has more affinity with one of the azeotropic components than with the others so as to draw the former along with it.

Heterogeneous azeotropic mixtures are nonideal mixtures characterized by the occurrence of at least one heterogeneous azeotrope. The latter is defined by two liquid phases in coexistence with a single vapor phase, the composition of which equals the overall liquid composition. Heterogeneous azeotropic distillation (HAD) refers to the distillation process whereby the separation agent and the initial mixture form a heterogeneous azeotropic mixture. HAD is widely used in industry because it offers a good economic compromise through the easy separation of the two liquid phases in a decanter. However, liquid−liquid demixing can occur in the column and on the trays, and both understanding the behavior and controlling the process of HAD are difficult.[1,2]

* Author to whom correspondence should be sent. E-mail: Vincent.Gerbaud@ensiacet.fr.

[†] Laboratoire de Génie Chimique.

[‡] ProSim S.A.

[§] Centre Technique de Lyon.

In this article, a thorough study of an industrial process is presented. Its aim is to explain industrial process operation and control difficulties leading to unmet purity requirements. As the unmet purity requirements occurred after an increase in the production rate of the unit, a shift from a steady state to another state is strongly suspected as the cause, and we investigate whether theoretical analysis and simulation lead to the same conclusions. First, the difficulties commonly encountered in heterogeneous azeotropic distillation are briefly discussed. Then, the process is described. A third section focuses on the modeling aspects used in this study. In the fourth part, the equilibrium model is validated through the simulation of a pilot unit that was specifically designed to capture the main operating features of the process main column. In the fifth part, multiple steady states found by simulation for the pilot unit are discussed and are related to instabilities observed during the pilot experiments. Finally, the industrial process operation is simulated as a two-column sequence: multiple steady states are predicted by the theoretical analysis, confirmed by simulation, and related to industrial data. Explanations of the control difficulties encountered in industrial practice are discussed.

2. Scope of the Paper

Industrial management of heterogeneous azeotropic distillation is difficult. Widagdo and Seider[1] have re-

viewed azeotropic distillation, and in particular, they cited the following key features of HAD as being connected with difficulties: (1) HAD design offers many possibilities both in the choice of a separation agent and in the process structure (column sequence order and recycling location). This choice extends the conceivable combinations and makes the design more difficult to perform efficiently. (2) The column behavior is not well-known. An explanation might be the occurrence of steady-state multiplicity. (3) Because the behavior is not well understood, the control of such columns is very difficult and is mainly based on practitioners' know-how.

A frequent observation made in HAD process units is that slight variations in impurity concentrations in the azeotropic column bottom output are correlated with big operating differences substantiated through large changes in tray temperatures and composition.[3,4]

For the industrial unit on which we base this study, practice has also shown that large changes in the temperature profile can occur and are related to variations in the concentrations of impurities in the bottom stream. These variations take place even though the controller set points remain unchanged. In adddition, there is evidence that the column composition profile of the industrial unit shifts after an increase in the unit production rate. One might ask whether these phenomena are related to the existence of multiple steady states that have been known to occur in other HAD processes.[1,5] "Multiple steady states" (MSS) usually refers to the multiplicity of solutions for systems of nonlinear equations used for steady-state simulation, when these solutions belong to the physical domain. This phenomenon is not only a mathematical feature as it has been experimentally demonstrated.[6−9] MSS are usually classified in the three following categories:[10,11] (1) input multiplicity occurs when multiple input values exist for a given set of outputs, (2) output multiplicity occurs when multiple output values exist for a given set of inputs, and (3) state multiplicity occurs when multiple output values of internal states exist for a given set of inputs and outputs.

It is important to note that this classification depends on the definitions of inputs and outputs, which refer to simulation or even to ∞/∞ analysis (described in Bekiaris et al.[12]). Generally, column inlet flow rates and compositions are fixed; some flow rates (of reflux and of distillate for example) are parameters called inputs, and the compositions of the column outlets are outputs. The study of input MSS is mainly used for design, whereas the study of output and state MSS is used for understanding behavior. Because we study an existing unit, we consider output MSS.

Doherty and Perkins[13] have shown the uniqueness of solution for ideal binary distillation defined by molar parameters with a constant molar overflow (CMO). Apart from steady-state multiplicity due to numerical tolerances that are too loose[14] or to thermodynamic phase equilibrium models,[11,15] three causes of output MSS for a single column have been identified:[6,11] (1) the nonlinear transformation between volumetric or mass flow rates and molar flow rates,[16] which has been experimentally validated by Kienle et al.;[6] (2) the interactions between molar overflows and their compositions with potential opposite influences of the material and the energy balances;[16] and (3) phase equilibrium properties of azeotropic mixtures with an influence of the mixture type in the vicinity of stable and unstable

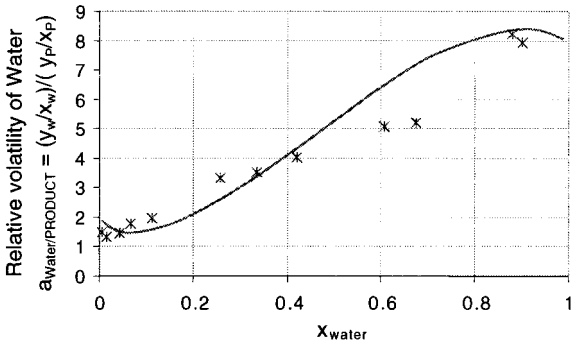

Figure 1. Water−product relative volatility curve: —, NRTL model; *, data from DECHEMA.

nodes.[17,18] The ∞/∞ analysis can be used in this case. This has been experimentally validated for homogeneous azeotropic distillation by Güttinger et al.[8] and for heterogeneous azeotropic distillation by Müller and Marquardt.[9]

The first two causes can be found in any kind of distillation, even in ideal binary ones, whereas the last case concerns only nonideal mixtures with homogeneous or heterogeneous azeotropes. The first and third causes can be found with constant molar overflow (CMO) models, whereas the second is based on molar overflow variations.

Extractive distillation processes usually involve a two-column sequence,[19] including an extractive column and a solvent recovery column. Taking into account the solvent recovery column is quite important because MSS can arise from the column sequence. Sequences are different from classical interconnected columns, whose multiplicity has been studied by Lin et al.[20] Güttinger and Morari[21] studied a homogeneous azeotropic distillation column connected to a solvent recovery column for several configurations and mixtures. Esbjerg et al.[10] studied a heterogeneous azeotropic distillation column connected to a solvent recovery column for direct and indirect sequences. They found multiple steady states that correspond to column concentration profiles located in different distillation regions.

Apart from Kovach and Seider,[3] very few studies of industrial units have been published. We intend, in this paper, to work out the peculiar behavior observed in an industrial unit through a systematic approach: validation of the simulation model in a pilot unit, investigation by ∞/∞ analysis, and simulation of multiple-steadt-state occurrences for the pilot unit and for the industrial unit. Consequences for the industrial unit operation are drawn accordingly.

Numerical values are presented using relative units. For example, temperature is graded with respect to a sensitive tray temperature set point. Boiler heat duty refers to a nominal value. Recovery rates are used for the stream main components. Mass fractions are used only for trace components.

3. Descriptions of the Industrial Process Unit and Pilot Column

3.1. Industrial Unit. The aim of the industrial process is the dehydration of an organic acid. For the purpose of simplifying the study, we consider the quaternary heterogeneous azeotropic system water−product−byproduct−solvent.

Figure 1 shows the evolution of the water−product relative volatility curve with the water molar fraction.

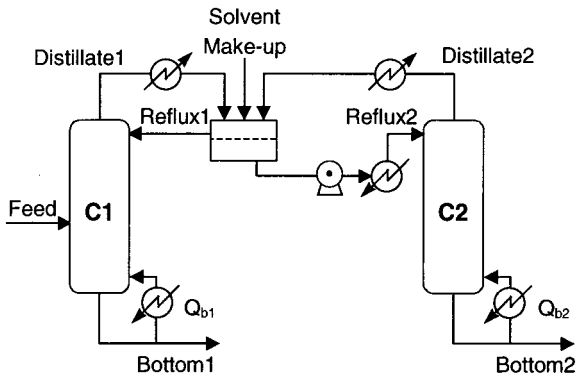

Figure 2. Industrial unit: simplified process used for the simulation.

As the experimental volatility is very close to unity near the pure-water locus (Figure 1), direct distillation is not appropriate for the recovery of a high amount of the product. The industrial process consists of adding an organic solvent that makes a heterogeneous azeotrope with water.

The industrial process is sketched in Figure 2. It consists of a heterogeneous azeotropic distillation column (C1) and a solvent regenerating column (C2), linked by a common decanter. High-purity product is collected in the bottom stream of the C1 column, whereas the minimum-temperature water−solvent heterogeneous azeotrope exits at the top of C1. This latter stream is input into the decanter. The decanter aqueous phase is fed entirely to the solvent-regenerating column (C2), where high-purity water is collected at the bottom and solvent is recycled to the common decanter. The decanter organic phase is refluxed to the azeotropic tower. A small makeup stream of solvent is necessary to replace small losses in the C1 bottom stream (bottom1, mainly product) and the C2 bottom stream (bottom2, mainly water). A sensitive tray is selected in the lower part of column C1, and its temperature is used as a reference point for the control loop.

3.2. Measurements and Control Systems of the Industrial Unit. Industrial process operation and control difficulties leading to unmet purity requirements have been observed after an increase in the unit production rate. Before the increase, the experimental data that we denote run ind_a met the purity requirements in terms of low water and solvent contents in the bottom1 stream. The column temperature profile is not available for run ind_a, but a few tray composition data in column C1 are available. The industrial test run called run ind_b does not meet the purity requirements in the bottom1 stream. It provides no tray composition data, but nevertheless it offers a more complete set of data than run ind_a, including the stream flow rates and compositions through the whole process, the temperatures on 10 trays (including decanter and boiler) of column C1 and 4 trays (including decanter and boiler) of column C2; the top and bottom pressures of columns C1 and C2, and the pressure level in the decanter.

The control system of the process aims at meeting the solvent and water content requirements in the bottom1 stream and maximizing the recovery yield of the product. For each column, the control loop consists of a measurement of the temperature on a selected sensitive tray and a suitable action on the device controlling the boiler heat duty.

3.3. Pilot Unit. Measurements obtained on the industrial process are not complete enough for the purpose of understanding the unit behavior. Therefore, a pilot unit was built and used to obtain the information necessary for assessing the validity of the simulation model. Using a synthetic four-component feed further decreases the study complexity. The pilot unit layout is shown in Figure 3. It consists of an azeotropic tower alone with a decanter. The number of trays is set in order to adequately model the industrial column behavior. The input and output streams are connected to storage tanks. For technical reasons, the organic phase is not directly refluxed in the column but rather is conveyed first through a storage tank and then into the column. Because the residence time in the storage tank is too long, this technical choice prevents us from reaching a full steady state during the data acquisition period. As in the industrial unit, a sensitive tray is selected in the lower part of the pilot column, and its temperature is used as a reference point. This temperature value is chosen by the operators so as to obtain an almost-pure product stream in the bottom of the column.

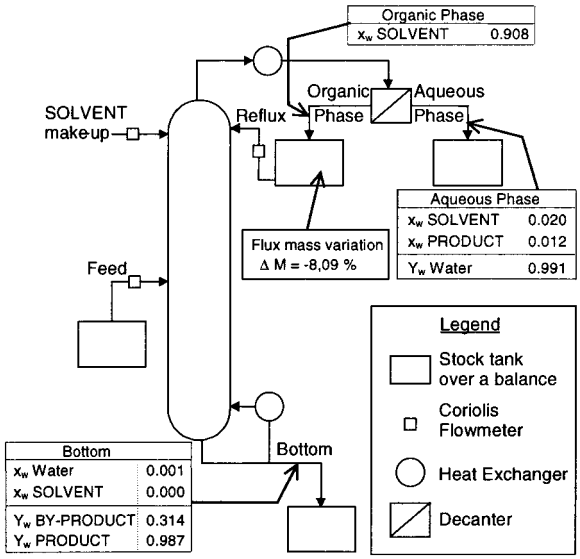

Figure 3. Pilot unit structure and key reconciled experimental data of the run pilot_a experiments.

3.4. Measurements and Control Systems of the Pilot Unit. For the pilot unit, the compositions and flow rates of the three input streams and of the three output streams are continuously recorded by computer. Temperatures are measured on seven trays. The experimental input and output stream composition and flow rate data are reconciled according to the approach of Meyer et al.[22] to satisfy partial and total material balances. Two experimental data runs are used in this study, namely, run pilot_a and run pilot_b. Some reconciled recovery rates and compositions typical values for run pilot_a are shown in the pilot layout (Figure 3) and are used as our reference set of experimental data. Run pilot_b differs from run pilot_a in that it has a higher set point for the sensitive tray reference temperature. Indeed, steady state could not be reached for run pilot_b with the set point reference temperature of run pilot_a, and operators had to shift the set point reference temperature 3 °C upward.

4. Validation of the Simulation Model

4.1. Description of the Simulation Model. The simulation study is performed with the case study tool ProCase,[23] which is based on a second-order polynomial

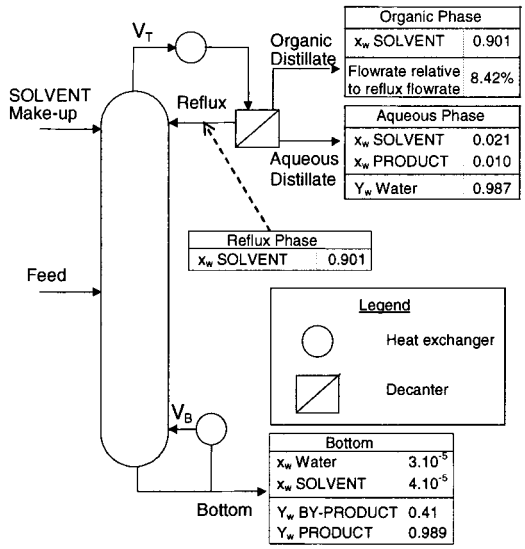

Figure 4. Pilot unit simulation layout and key results from the simulation.

continuation method. This tool follows an operating path, which is defined as a succession of steady states characterized by continuously derivable output results; it provides a reasonable model for the process behavior when an operating parameter is varied. Convergence and operating paths are readily reached because each new steady-state solution is obtained using the previously converged steady-state results for the initializing conditions. This tool can also detect multiple solutions that belong to different operating paths either starting from a new value of the operating parameter or restarting with a direction given by converged simulations that do not belong to the previously calculated operating path.

Liquid−vapor equilibrium (LVE) and liquid−liquid−vapor equilibrium (LLVE) are described by the equality of phase fugacities. The liquid fugacities are calculated using the NRTL thermodynamic model with temperature-dependent binary coefficients.[24] Binary coefficients were identified using binary experimental data at the proper pressures. The consistency of all of the thermodynamic data was carefully checked as it has been recently shown to be critical for the simulation of MSS phenomena.[11]

The steady-state distillation column model[25] consists of the usual MESH (material balance, liquid−liquid−vapor equilibrium, summation of fractions, and heat balance) equations. Molar units are used. Because spurious MSS can appear in simulations when insufficiently stringent convergence criteria are used,[14] tighter-than-usual convergence criteria values are set (10^{-12} instead of 10^{-8}).

4.2. Simulation of the Pilot Column. The behavior of the heterogeneous azeotropic column is assessed using the steady-state simulator in combination with the case study tool described above. The pilot unit layout used for the simulation is presented in Figure 4, along with typical recovery rate and composition values from the simulation of run pilot_a. Default (surplus) of the organic phase in the storage tank is represented in a steady-state way by an inlet (outlet) stream of organic phase. This can be done because the experimental material reduction (accumulation) in the storage tank does not affect significantly the compositions of the distillate and reflux streams. In addition, the measured

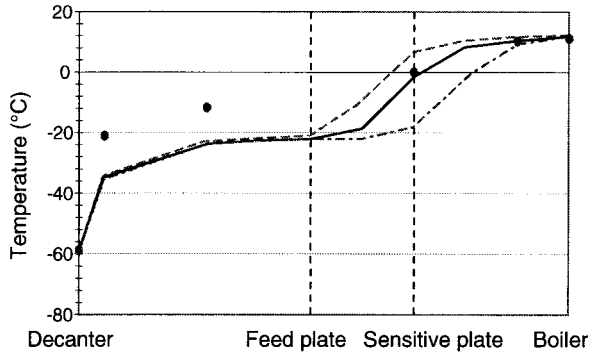

Figure 5. Comparison of experimental and simulated column temperature profiles. Sensitivity of the profile to the boiler heat duty (temperature graded with respect to the sensitive tray temperature set point) for run pilot_a: ●, experimental; —, nominal Q_b; − − −, Q_b − 0.23%; - − -, Q_b + 0.23%.

composition values are averaged before being reconciled, thus smoothing further the impact of the reduction or accumulation in the storage tank. The MESH equations leave three degrees of freedom that must be satisfied. A zero heavy reflux flow rate, the boiler duty, and a zero light distillate flow rate are chosen as operating parameters. As we do not know the boiler duty because of unknown heat losses within the heating fluid circulation loop, our interest in using the boiler duty as an operating parameter for the sensitivity analysis performed with the case study tool is reinforced.

4.3. Validation of the Model by Comparison of Pilot Experimental Data with Simulation Results. The boiler duty value was varied at constant molar reflux flow rate, and the resultant steady-state solutions were analyzed. Simulated temperature profiles in the pilot column for three boiler duty values along with experimental temperature measurements are shown in Figure 5. We notice that two types of temperature profiles in the column, low and high, are seen over a small (0.46%) variation of the Q_b range. The agreement between the experimental and simulated temperatures is always good on the feed tray and on the boiler (the agreement is good on the condenser because the temperature is fixed a priori during the simulation). As the boiler duty increases, the temperature in the lower part of the column increases, whereas the temperature does not change in the upper part of the column. The discrepancy between the experimental and simulated temperature profiles in the upper part of the column could be explained by the default adiabatic model used for tray simulation (we do not know the heat losses), which concentrates the cooling on the condenser.

The boiler duty that corresponds to the best temperature profile agreement is denoted Q_b nominal (see Figure 5). Computed with the Q_b nominal value, experimental versus simulated errors in the concentrations and flow rates of the output streams are presented in Table 1. As the low error values show, the experimental and simulated concentrations and flow rates are in good agreement, especially if we consider the modeling approximation that converts the storage tank accumulation to a process output flow rate (organic distillate). Therefore, the pilot simulation validates both the MESH steady-state simulation model and the liquid−liquid−vapor equilibrium (thermodynamic) model in terms of physically coherent results.

4.4. Pilot Column Behavior. The sensitive temperature profile shift suggested in Figure 5 offers some

Table 1. Comparison of Reconciled Experimental Outlets and Simulated Outlets for Nominal Boiler Duty Q_b: Absolute Error in Composition, Relative Error in Flow Rate for the Pilot Unit, Run Pilot_a

		errors (simulated vs experimental)		
		organic distillate	aqueous distillate	bottom
mass fraction	water	+0.011	+0.004	-6.97×10^{-4}
	product	+0.002	−0.002	−0.002
	byproduct	-0.010	−0.003	+0.003
	solvent	−0.003	+0.001	-1.60×10^{-4}
mass flow rate		−0.2%	−0.6%	+0.4%

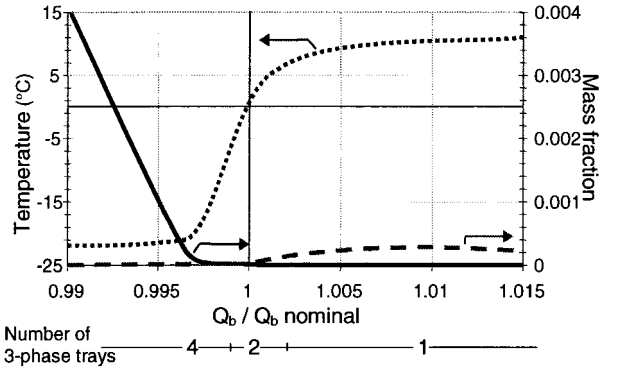

Figure 6. Comparison of the simulated variations of the pilot column sensitive tray temperature and column bottom outlet impurity compositions with boiler duty (Q_b/Q_b nominal) for run pilot_a: ···, sensitive plate temperature graded with respect to the run pilot_a nominal temperature set point; —, water fraction; – – –, solvent fraction.

insight into the column behavior. Figure 6 displays the variation of the sensitive tray temperature and of the solvent and water contents in the product-rich column bottom stream with respect to the boiler duty value. The shift between the two temperature profiles is sharp, as the temperature of the sensitive tray experiences a 25 °C jump over a 0.46% variation of the boiler duty. This readily explains the choice of this particular tray temperature as a control parameter. The sharp temperature increase is accompanied by a steep decrease in the water content in the bottom stream, whereas the solvent content in the bottom stream first increases up to a concentration maximum and then diminishes (Figure 6). Therefore, the chosen sensitive tray reference temperature value corresponds to a minimum in the impurity concentration of the product-rich bottom stream.

According to Figure 6, operating at high Q_b value with a high temperature profile seems acceptable on the basis of the impurity content in the product-rich bottom stream. Unfortunately, however, it greatly impairs the product and byproduct mass yield, as shown in Figure 7. Indeed, the product recovery value decreases and falls below the 95 wt % target value when Q_b > 1.01(Q_b nominal).

Notice that the almost perfectly symmetrical variations in the byproduct recovery value and sensitive tray temperature displayed in Figure 7 are a coincidence, as the same simulation procedure made without byproduct gives a similarly abrupt sensitive tray temperature profile (see Figure 8). Finally, we notice in Figure 6 that the number of heterogeneous trays varies from four when the temperature profile is low to a single one (the decanter) for the high temperature profile. The increasing presence of byproduct and product on the upper

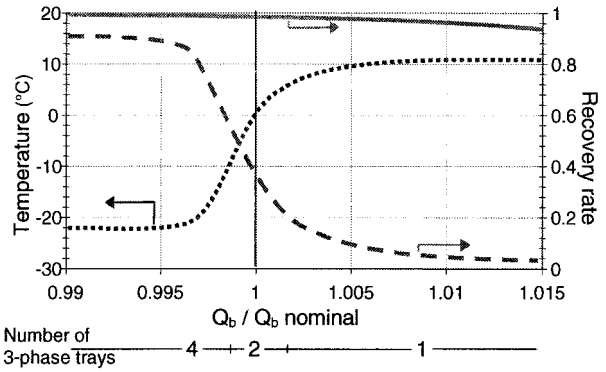

Figure 7. Comparison of the simulated variations of the sensitive tray temperature and recovery rate in the bottom product with boiler duty (Q_b/Q_b nominal) for run pilot_a: ···, sensitive tray temperature graded with respect to the run pilot_a nominal temperature set point; – – –, byproduct recovery rate; —, product recovery rate.

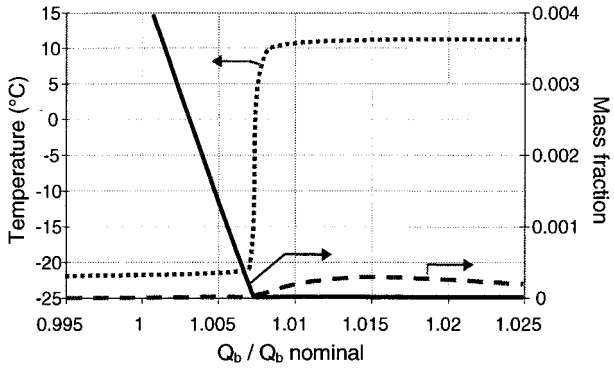

Figure 8. Simulation without byproduct of the variations of the sensitive tray temperature and the column bottom outlet impurity composition with boiler duty (Q_b/Q_b nominal) for run pilot_a: ···, sensitive tray temperature graded with respect to the run pilot_a nominal temperature set point; —, water fraction; – –, solvent fraction.

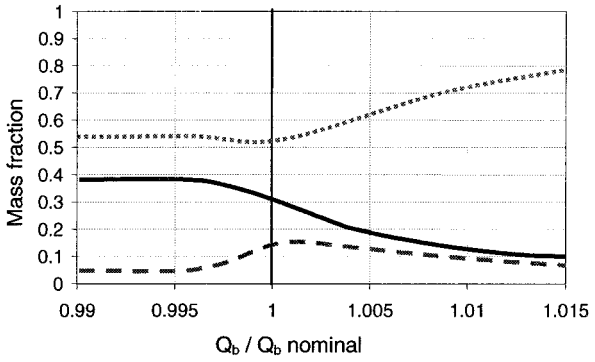

Figure 9. Simulation of the variation of the mass fraction in a tray located in the upper part of the column versus boiler duty (Q_b/Q_b nominal) for run pilot_a: —, water; ···, product; – – –, byproduct.

trays sets the liquid mixture away from the demixing zone, which concerns mostly water and solvent compounds.

Figures 9 and 10 display the simulation results for the evolution of the mass fractions of product, byproduct, and water with Q_b for two significant trays, one located above the main feed stream and the other located below the feed and acting as the sensitive tray. As Q_b goes up, water is removed from the bottom of the column. Once the bottom stream is almost depleted of water, the byproduct starts moving up the column,

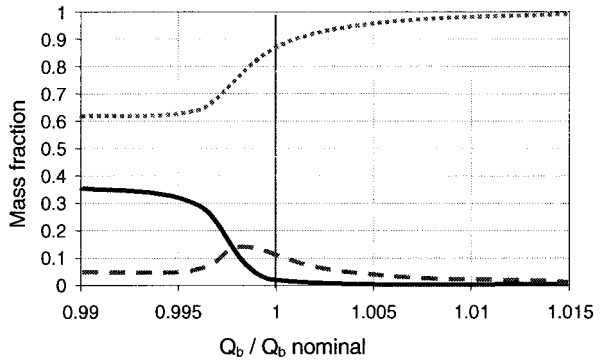

Figure 10. Simulation of the variation of mass fraction in the sensitive tray versus boiler duty (Q_b/Q_b nominal) for run pilot_a: —, water; · · ·, product; — — —, byproduct.

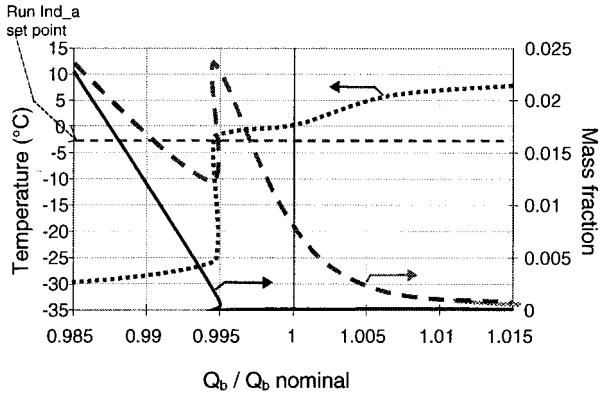

Figure 11. Simulation of the variations of the sensitive tray temperature and column bottom outlet impurity composition with boiler duty (Q_b/Q_b nominal) for run pilot_b: · · ·, sensitive tray temperature graded with respect to the run pilot_b nominal temperature set point; —, water fraction; — — — solvent fraction.

followed by the product. These moving concentration fronts can be set in parallel with a moving temperature front (Figure 5).

As a conclusion for the pilot unit simulation, the simulation shows that either a high or a low temperature profile in the lower part of the column exists. A shift from one profile to the other corresponds to an inversion of the impurity concentration in the bottom stream. The experimental profile lies between the two simulated profiles. It is characterized by a sensitive tray temperature set point that, according to the simulation, corresponds to an impurity concentration minimum in the product-rich bottom stream. Such a minimum is looked after by the operators that choose the sensitive tray temperature set point. Such results validate the simulation and thermodynamic models that are used for the simulation of the industrial unit.

5. Multiple Steady States due to Nonconstant Molar Overflows in the Pilot Unit

5.1. Display of Multiple Steady States. A similar pilot unit simulation study was performed for another experimental campaign (run pilot_b) in which operators had to shift the sensitive tray temperature set point upward. It shows the same kind of large variation of the sensitive tray temperature over a restricted range of boiler duty (see Figure 11). Moreover, the analysis of this second pilot simulation shows some multiple steady states in a boiler duty operation range close to the

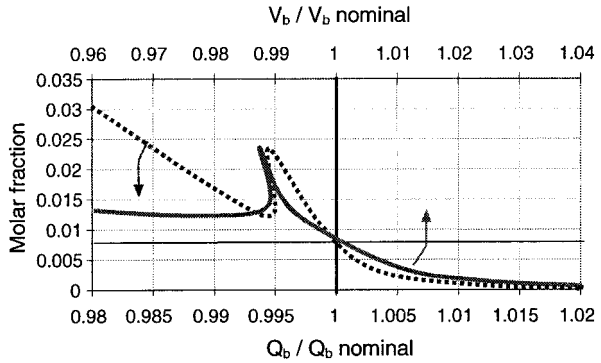

Figure 12. Multiple steady states for Q_b and for molar parameter V_b for run pilot_b: - - -, solvent molar fraction versus boiler duty (Q_b/Q_b nominal); —, solvent molar fraction versus molar vapor flow rate in the bottom of the column (V_b/V_b nominal).

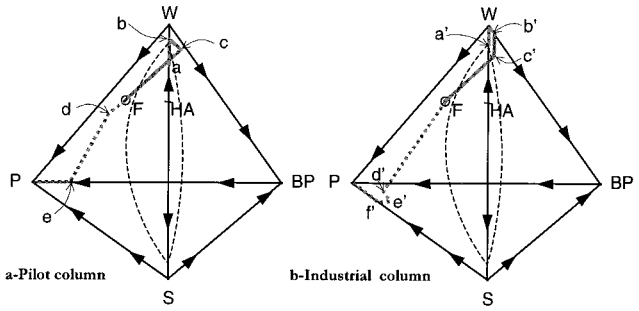

Figure 13. ∞/∞ analysis diagrams for the quaternary mixture solvent (S)−product (P)−byproduct (BP)−water (W). HA stands for the water−solvent heterogeneous azeotrope. (a) pilot column: —, distillate composition path abcF; · · ·, bottom composition path FdeP. (b) industrial column: —, distillate composition path a′Wb′c′F; · · ·, bottom composition path Fd′e′f′P.

Table 2. Comparison of Run Ind_b Experimental Outputs Versus Simulated Outputs for Various Stream Compositions and Flow Rates for Q_{b1} and Q_{b2} Nominal, Industrial Unit

absolute errors in mass fraction				
	bottom1		bottom2	
	SS1	SS2	SS1	SS2
product	+0.991	+0.021	−0.0005	+0.0004
water	−2583 ppm	−2586 ppm	+0.009	−0.020
byproduct	+0.003	+0.018	−0.005	+0.023
solvent	−47 ppm	−45 ppm	−91 ppm	−91 ppm
relative errors on mass flow rate				
	column c1		column c2	
	SS1	SS2	SS1	SS2
distillate	+0.113	+0.061	−0.327	−0.280
reflux	+0.139	+0.063	+0.020	+0.023
bottom	−	−0.022	−0.003	−0.026

operating range, as shown in Figure 12. In addition, these multiple steady states are sensitive to the main feed flow rate value: a variation of less than 2% increases the arrival or the removal of the unstable region and the multiple steady states (not shown).

5.2. Hypothesis for the Multiple Steady States Observed. Because the continuation parameter is the boiler duty, the cause for the multiple steady states might be the nonlinear transformation between the parameter and molar flow rates. However, this is not the essential reason as there are still some multiple steady states if the operating parameter is the molar flow rate of vapor leaving the boiler, V_b (see Figure 12, top axis).

Table 3. Information along the Continuation Path for the Pilot Column ∞/∞ Analysis of the Heterogeneous Azeotropic Column with Decanter for the Quaternary System Water−Byproduct−Solvent−Product

pinch point	HA	HA		W		BP		P	P
corresponding figure 18	i		ii		iii		iv		v
$x_{distillate}$ path	a		a	→	b	→	c	→	F
x_{bottom} path	F	→	d	→	e	→	P		P
distillate flow rate	0	↑	$W' + S$	↑	$W + S$	↑	$W + S + BP$	↑	F
x_D value	x_A	↑		↑		↓		↓	x_F

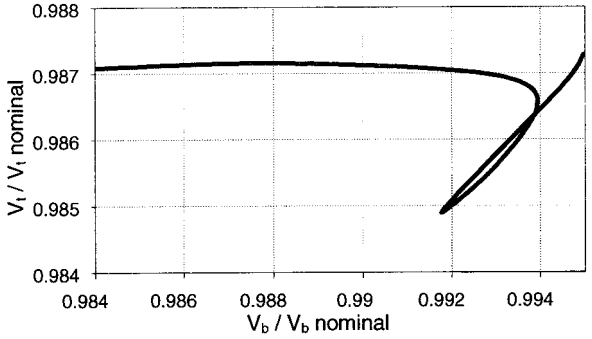

Figure 14. Variation of the vapor flow rate at the top of the column (V_t/V_t nominal) versus vapor flow rate at the bottom (V_b/V_b nominal) for run pilot_b.

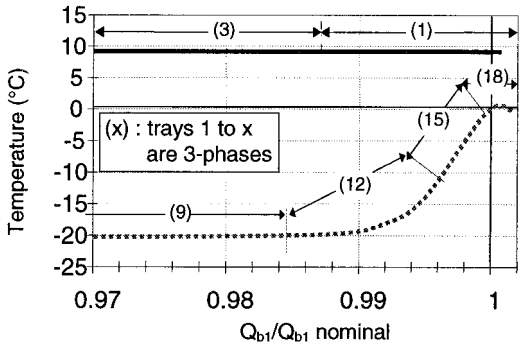

Figure 15. Multiple operating paths for the industrial unit [sensitive tray temperature graded with respect to the industrial nominal temperature set point versus boiler duty (Q_{b1}/Q_{b1} nominal)]: - - -, SS1; —, SS2.

Then, an ∞/∞ analysis following the procedure for a heterogeneous mixture with a decanter[5,17] is performed. For the quaternary system water−byproduct−solvent−product, the unstable node is the binary heterogeneous azeotropic mixture, and the stable node is the product (P), whereas the byproduct (BP), the solvent (S), and the water (W) are saddle nodes. Following the classification of azeotropic mixtures of Matsuyama and Nishimura[26] adapted for heterogeneous mixtures by Matsuyama,[27] the mixtures W−S−P and W−S−BP are classified 100 and display a water−solvent heterogeneous azeotrope (HA), and the mixtures BP−S−P and W−BP−P are classified 000. The ∞/∞ analysis does not show any multiple steady states. Figure 13a and Table 3 show the distillate continuation path abcF, and the corresponding bottom line is FdeP. Details of the construction of Figure 13 are given in Appendix 1. Note that, for the pilot column, the global distillate is a combination of all of the decanter aqueous phase and some of the decanter organic phase, the latter being present so as to model the accumulation in the reflux storage tank. Therefore, point a in Figure 13a is located inside the demixing zone, and point d belongs to the P−W−BP composition triangle. As summarized in Table 3, the distillate flow rate grows continuously from 0 to $W' + S$, to $W + S$, to $W + S + BP$, and finally to the feed flow rate $F = W + S + BP + P$. Therefore, no intermediate decrease in the distillate flow rate that would evidence some multiple steady states is observed, and the geometric condition for MSS occurrence[17] does not occur here. As stated later, the ∞/∞ analysis made on the same quaternary system predicts multiple steady states for the industrial column, because the distillate is made of the sole decanter aqueous phase. The difference in the ∞/∞ analysis conclusions for the pilot and industrial columns was quite unexpected as the pilot column was supposedly built to reproduce the industrial unit behavior.

Despite the ∞/∞ analysis results for the pilot column, as stated by Bekiaris et al.,[17] the assumption of multiple steady states due to phase equilibrium properties cannot completely be excluded because the system is complex and does operate under finite/finite conditions. Nevertheless, the most probable cause of multiple steady states remains the nonconstant molar overflow due to the contrary influence of the material and energy balances on the flows and compositions. Indeed, as described by Jacobsen and Skojestad[16] in the case of constant reflux, the simulation shows a derivative $(\partial V_t/\partial V_b)_R$ that might be negative (see Figure 14) and then generates state multiplicity. This means that, in the unstable region, the increase in the vapor flow rate at the bottom of the column, V_b, is related to the increase in the liquid flow rate at the bottom of column, B, and to the decrease in the vapor flow rate at the top of the column, V_t.

Table 4. Comparison of Run Ind_a Experimental Versus Simulated Results of the Sensitive Tray Liquid Compositions for Q_{b1} and Q_{b2} Nominal, Industrial Unit

absolute errors in mass fraction		
	sensitive tray	
	SS1	SS2
product	−0.2269	+0.0107
water	+0.1312	+341 ppm
byproduct	+0.0885	−0.0081
solvent	−2991 ppm	−2976 ppm

5.3. Validation of the Multiple-Steady-States Hypothesis. Comparing run pilot_a and run pilot_b, the set point for the reference temperature has been shifted by 3 °C for run pilot_b because a steady-state could not be reached for the operating conditions of run pilot_b with the set point from run pilot_a. Figure 11 shows that the run pilot_b set point belongs to the stable region, whereas the usual reference set point for run pilot_a belongs to the unstable region. From this experimental instability, we infer the existence of an unstable region and the reality of multiple steady states.

6. Multiple Steady States in the Industrial Unit

6.1. Description of the Simulation Study of the Industrial Process. The simulation of columns C1 and C2 together retains the main features of the industrial

Table 5. Information along the Continuation Path for the Industrial Column ∞/∞ Analysis of the Heterogeneous Azeotropic Column with Decanter for the Quaternary System Water−Byproduct−Solvent−Product

pinch point	HA		HA		W					P		P	P
corresponding figure 19	i		ii			iii		iv		v			vi
$x_{distillate}$ path	a′		a′	→	W	→	b′	→	c′		→		F
x_{bottom} path	F	→	d′	→	e′	→	f′	→	P				P
distillate flow rate	0	↑	$W + S'$	↓	W	↑	$W + BP$	↑	$S + W + BP$		↑		F
x_D value	x_{Az}	↑		↑		↓		↓			↓		x_F

plant (see Figure 2). The pressure level and pressure drop are set according to experimental data. Because the liquid−liquid separation in the decanter automatically determines the reflux flow rates, only two independent input parameters must be specified for the two-column sequence. In the industrial process, the boiler duties are used to control the temperature of the sensitive tray for each column, and the heat power provided to each column is known with a low accuracy. That is why the two boiler duties are chosen as the industrial process simulation input parameters whose variations are studied. The solvent makeup represents the solvent added to balance the few losses that occur in the bottom of the two columns. For all of the presented cases, the value of the solvent makeup at convergence is zero even if its initial value or its value at convergence is not. This could be explain by the fact that the order of magnitude of the experimental solvent loses is comparable to that of the numerical errors.

The procedure of tracking an operating path performed with the case study tool using the C1 boiler duty (Q_{b1}) as the operating parameter gives two paths. This implies that two steady states for each Q_{b1} value exist (see Figure 15). The first path, SS1, is obtained for simulations that start the tracking procedure with any high value of Q_{b1}. The second path, SS2, is obtained starting with low values of Q_{b1}. For this path, we could not obtain simulation convergence for Q_{b1} higher than 1.01(Q_{b1} nominal). The convergence is already difficult for 1.005(Q_{b1} nominal). The importance of the initialization strategy for the simulation aimed at finding bifurcation points has already been pointed out in the literature.[28]

Attempts to follow an operating path with Q_{b2} as an operating parameter proved to be unsatisfactory because of the behavior described in section 6.4. Thus, we followed operating path with Q_{b1} as a parameter for various Q_{b2} values.

6.2. ∞/∞ Analysis for the Industrial Heterogeneous Azeotropic Column. An ∞/∞ analysis similar to that performed for the pilot unit was performed, but in this case, only the decanter aqueous phase was removed as distillate instead of a combination of the decanter aqueous and organic phases. The water fraction of a′ (Figure 13b, industrial column) is lower than the water fraction of a (Figure 13a, pilot column), and point d′ belongs to the P−BP−S composition triangle (d for the pilot belongs to the P−W−BP composition triangle). Therefore, the distillate and bottom paths are different for the pilot column and for the industrial unit. The distillation a′Wb′c′F and bottom Fd′e′f′P paths are shown in Figure 13b and Table 5 (details in Appendix 1). As the distillate flow rate decreases from $W + S'$ to W, multiple steady states are predicted by the ∞/∞ analysis. Therefore, the MSS occurrence in the industrial unit is due to the properties of the phase equilibrium. The MSS prediction for the heterogeneous azeotropic column will, of course, persist when the solvent recovery column is taken into account, as is the case in our simulation.

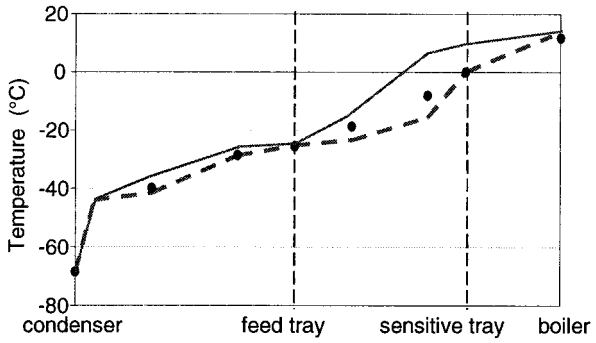

Figure 16. Temperature profiles (temperatures graded with respect to the sensitive tray temperature set point) for the industrial unit: ●, run ind_b experimental data; - - -, SS1; —, SS2.

6.3. Comparison of Experimental and Simulated Results for Both Steady States. The ∞/∞ analysis prediction of multiplicity is corroborated by a comparison of the experimental and simulation results. We managed to obtain a single pair of boiler duty values (called Q_{b1} nominal and Q_{b2} nominal) that gave good overall agreement between both simulated steady states SS1 and SS2 and the run ind_b experimental temperature profiles, as shown in Figure 16. For each steady state, the errors between run ind_b industrial measurements and the simulation results for the compositions and flow rates of the output streams are displayed in Table 2. Differences between the two simulated steady states occur in the reflux flow rates and compositions values of both columns, whereas the shift in the temperature profiles is significant below the feed tray between both steady states.

A closer look at Figure 16 shows that the best temperature profile matching is obtained for SS1. We can then conjecture that the simulated SS1 state corresponds to the run ind_b operation of the industrial unit. Table 4 displays a comparison of the run ind_a experimental and simulated results for the sensitive tray liquid compositions for Q_{b1} and Q_{b2} nominal. The agreement between the simulation and the run ind_a experimental sensitive tray composition is quite good for SS2 but very bad for SS1, which has too much water and byproduct and not enough product on the sensitive tray. Therefore, SS2 likely corresponds to run ind_a, which occurred before the feed flow rate increase that disturbed the product purity requirements.

The discrepancy in Tables 2 and 4 between the experimental measurements and the simulated results for either steady state is significant for components appearing in small quantities (e.g., water and solvent in bottom1). This can be explained in three ways: (i) the industrial condenser is slightly undersized compared to the ideal condenser case that is modeled; (ii) other impurities are not modeled in the simulation, and they might have a significant influence on small quantities; and (iii) the thermodynamic model introduces difficulties in making accurate predictions both for the whole composition range and for part-per-million values (in

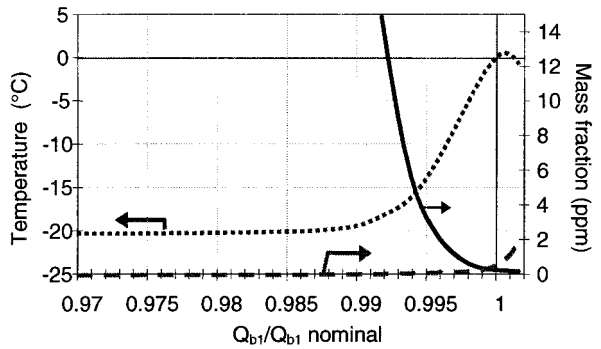

Figure 17. Variations in the temperature of the sensitive tray graded with respect to the industrial nominal temperature set point and in the bottom impurities compositions with column C1 boiler duty (Q_{b1}/Q_{b1} nominal) for SS1 of the industrial unit: ···, relative temperature; —, water fraction; − − −, solvent fraction.

the vicinity of infinite dilution). The dissimilarity between the experimental distillate and reflux flow rates and the simulated ones, despite the good agreement for the bottom streams bottom1 and bottom2, might arise from two modeling imperfections that compensate for each other: (i) as above for the industrial condenser and (ii) the industrial process is not totally adiabatic, which favors internal reflux at the expense of the distillate and reflux flow rates.

6.4. Explanation of the Process Behavior and Control Difficulties. In this paragraph, we analyze further the SS1 simulation results and relate them to the process behavior and control difficulties of run ind_b. Figure 17 shows the variation of the sensitive tray temperature and bottom impurities compositions with boiler duty Q_{b1} for SS1. We see a behavior similar to that observed during the pilot column runs: when the sensitive tray temperature is equal to the reference value, the total amount of impurities (water and solvent) in the bottom1 stream is a minimum. The water content has the same influence on the temperature profile, as a large amount of water in the column corresponds to a low-temperature profile.

However, three observations are different from the pilot study: (i) the variation of the column C1 sensitive tray temperature with Q_{b1} forms not a plateau but a peak, (ii) there are some convergence difficulties when Q_{b1} is greater than the Q_{b1} value corresponding to the peak, and (iii) the number of three-phase trays grows with Q_{b1} instead of diminishing.

When Q_{b2} is varied, the variation of the sensitive tray temperature with Q_{b1} has the same shape. However, the Q_{b1} value corresponding to the peak and the temperature maximum of the peak then vary with Q_{b2}.

The sharp variation of the temperature profile of the column and especially the temperature peak on the sensitive tray might explain the difficulties in controlling the process for the run ind_b industrial set point that lies close to the maximum of the peak: if Q_{b1} decreases, the temperature of the sensitive tray decreases, and if Q_{b1} increases, the temperature decreases as well. Furthermore, Q_{b2} variations change the peak Q_{b1} value, which enforces the control difficulties.

7. Conclusion

In this article, a study of a running industrial heterogeneous azeotropic distillation unit is presented. The study includes a validation of the MESH and thermodynamic models through a comparison between experimental and simulation results for a pilot column. The analysis of the behavior of this heterogeneous azeotropic distillation unit confirms the relationship between impurities in the bottom stream and the column temperature profile.

For the industrial unit sequence, simulation results display an unusual peak in the response of the azeotropic column sensitive tray temperature to variations in the heat duty. The control difficulties observed with the industrial unit might be caused by the choice of using an operating sensitive tray temperature set point close to the maximum of this peak. However, this choice is relevant because the simulation tells us that it is related to a minimum of impurity in the product-rich bottom stream.

An ∞/∞ analysis for the quaternary mixture is performed for the heterogeneous azeotropic pilot column and the industrial column with a decanter. As a result of practical constraints, the pilot and the industrial columns do not have the same reflux policy. This lead the ∞/∞ analysis to predict multiple steady states for the industrial unit but not for the pilot column. However, multiple steady states are found both for the pilot and industrial units. Simulation and experimental evidence for the industrial unit confirms the steady-state multiplicity. Because of the conclusive ∞/∞ analysis, these multiple steady states are attributed to phase equilibrium properties of the quaternary system. For the pilot column, multiple steady states are found by the simulation and are linked to the experimental observations. The cause of multiplicity is attributed not to the phase equilibrium properties but rather to interactions between the material and energy balances.

The next steps for this study are a sensibility analysis and a dynamic simulation to develop a control policy andto investigate the possible shifts from one steady state to another, in particular when a feed flow rate increase occurs.

Acknowledgment

The authors thank the reviewers for pointing out some incoherence in the first version of the paper that compelled us to investigate more deeply the theoretical analysis of the process behavior.

Notation

B = liquid flow rate at the bottom of the column
BP = byproduct flow rate
P = product flow rate
S, S' = solvent flow rate, solvent partial flow rate
W, W' = water flow rate, water partial flow rate
R = reflux flow rate
V_b, V_t = vapor flow rate at the bottom, top of the column
Q_b = boiler duty
x_w = liquid weight fraction
x = liquid molar fraction
y = vapor molar fraction
Y_w = weight yield/recovery rate

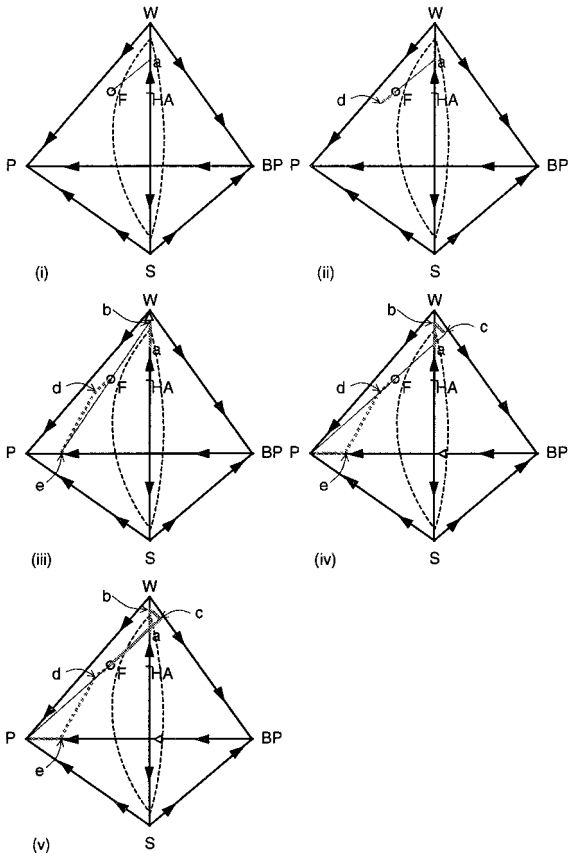

Figure 18. Pilot column ∞/∞ analysis for the quaternary mixture solvent (S)−product (P)−byproduct (BP)−water (W). HA stands for the water−solvent heterogeneous azeotrope: −, distillate composition path abcF; · · ·, bottom composition path FdeP; —, column balance line.

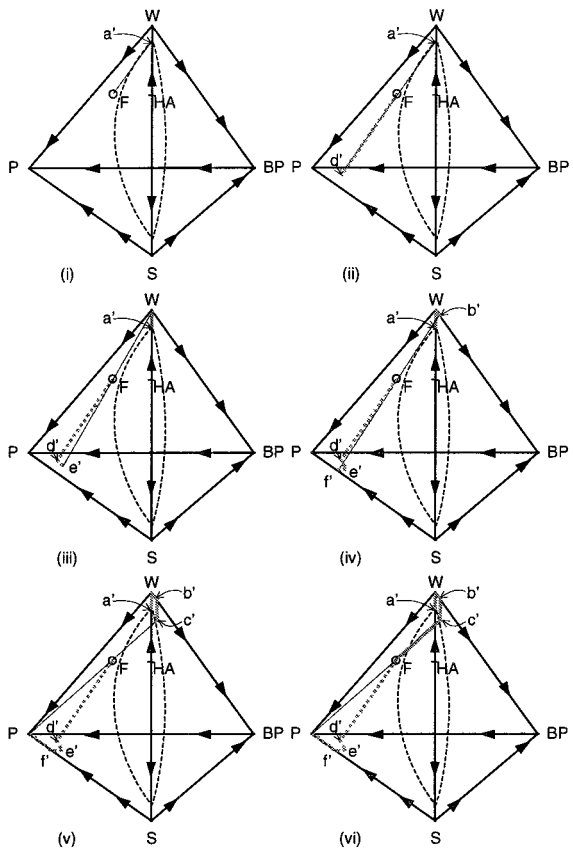

Figure 19. Industrial column ∞/∞ analysis for the quaternary mixture solvent (S)−product (P)−byproduct (BP)−water (W). HA stands for the water−solvent heterogeneous azeotrope: −, distillate composition path a′Wb′c′F; · · ·, bottom composition path Fd′e′f′P; —, column balance line.

Appendix 1

∞/∞ analysis is a valuable tool that provides a simple physical explanation, as well as a graphical prediction method, for the occurrence of output multiplicities due to phase equilibrium properties. It relies on two assumptions. First, an infinite reflux allows distillation lines and residue curves to merge. Second, an infinite number of stages ensures that the distillation line will pass by at least one node (pinch point). Notice that a conclusive ∞/∞ analysis is a sufficient but not necessary condition for output multiplicities to occur.[5,11] However, for a heterogeneous azeotropic column with a decanter, the reflux policy must be specified. The material balance still holds between the feed, the bottom, and the overhead vapor, but the true distillate composition, which might differ from the overhead vapor composition, must be taken into account when the distillate and bottom paths are determined.

For our particular study, the ∞/∞ analysis progression is shown in Figure 18 for the pilot column and in Figure 19 for the industrial unit. Information along the continuation path is outlined in Tables 3 and 5. For the pilot column, the overall distillate (point a in Figure 18) is made up of all of the decanter aqueous phase and a portion of the decanter organic phase (see Figure 4). In the industrial case, only the decanter aqueous phase is withdrawn as distillate (point a′ in Figure 19). The assessment of the proper distillate policy has some profound implications as the ∞/∞ analysis predicts MSS for the industrial unit but not for the pilot column.

Literature Cited

(1) Widagdo, S.; Seider, W. D. Azeotropic Distillation. *AIChE J.* **1996**, *42*, 96.

(2) CAPE-Net. http://capenet.chemeng.ucl.ac.uk.

(3) Kowach, J., III; Seider, W. Heterogeneous Azeotropic Distillation: Experimental and Simulation Results. *AIChE J.* **1987**, *33*, 1300.

(4) Pham, H. N.; Ryan, P. J.; Doherty, M. F. Design and Minimum Reflux for Heterogeneous Azeotropic Distillation Columns. *AIChE J.* **1989**, *35*, 1585.

(5) Bekiaris, N.; Meski, G.; Morari, M. Multiple Steady States in Heterogeneous Azeotropic Distillation. *Ind. Eng. Chem. Res.* **1996**, *35*, 207.

(6) Kienle, A.; Groebel, M.; Gilles, E. D. Multiple Steady States in Binary Distillation—Theoretical and Experimental Results. *Chem. Eng. Sci.* **1995**, *50*, 2691.

(7) Bauer, W.; Chapman, J. T. Process for producing alkyl acrylate. European Patent EP 0 779 268 A1, 1997.

(8) Güttinger, T.; Dorn, C.; Morari, M. Experimental Study of Multiple Steady States in Homogeneous Azeotropic Distillation. *Ind. Eng. Chem. Res.* **1997**, *36*, 794.

(9) Müller, D.; Marquardt, W. Experimental Verification of Multiple Steady States in Heterogeneous Azeotropic Distillation. *Ind. Eng. Chem. Res.* **1997**, *36*, 5410.

(10) Esbjerg, K.; Andersen, T.; Müller, D.; Marquardt, W.; Jørgensen, S. Multiple Steady States in Heterogeneous Azeotropic Distillation Sequences. *Ind. Eng. Chem. Res.* **1998**, *37*, 4434.

(11) Bekiaris, N.; Güttinger, T. E.; Morari, M. Multiple Steady States in Distillation: Effect of VL(L)E Inaccuracies. *AIChE J.* **2000**, *46* (5), 955.

(12) Bekiaris, N.; Meski, G.; Radu, C.; Morari, M. Multiple Steady States in Homogeneous Azeotropic Distillation. *Ind. Eng. Chem. Res.* **1993**, *32*, 2023.

(13) Doherty, M.; Perkins, J. On the Dynamics of Distillation Processes IV. Uniqueness and Stability of the Steady-State in Homogeneous Continuous Distillations. *Chem. Eng. Sci.* **1982**, *37*, 381.

(14) Rovaglio, M.; Faravelli, T.; Biardi, G.; Gaffuri, P.; Soccol, S. The Key Role of Entrainer Inventory for Operation and Control of Heterogeneous Azeotropic Distillation Towers. *Comput. Chem. Eng.* **1993**, *17*, 535.

(15) Van Dongen, D.; Doherty, M.; Haight, J. Material Stability of Multicomponent Mixtures and Multiplicity of Solutions to Phase-Equilibrium Equations. 1. Nonreacting Mixtures. *Ind. Eng. Chem. Fundam.* **1983**, *22*, 472.

(16) Jacobsen, E.; Skogestad, S. Multiple Steady States in Ideal Two-Product Distillation. *AIChE J.* **1991**, *37*, 499.

(17) Bekiaris, N.; Morari, M. Multiple Steady States in Distillation: Predictions, Extensions and Implications for Design, Synthesis and Simulation. *Ind. Eng. Chem. Res.* **1996**, *35*, 4264.

(18) Kienle, A.; Gilles, E.; Marquardt, W. Computing Multiple Steady States in Homogeneous Azeotropic Distillation Processes. *Comput. Chem. Eng.* **1994**, *18*, S37.

(19) Pham, H. N.; Doherty, M. F. Design and Synthesis of Heterogeneous Azeotropic Distillations. III. Column Sequences. *Chem. Eng. Sci.* **1989**, *45*, 1845.

(20) Lin, W.-J.; Seader, J. D.; Wayburn, T. L. Computing Multiple Solutions to Systems of Interlinked Separation Columns. *AIChE J.* **1987**, *33*, 886.

(21) Güttinger, T.; Morari, M. Multiple Steady States in Homogeneous Separation Sequences. *Ind. Eng. Chem. Res.* **1996**, *35*, 4597.

(22) Meyer, M.; Koehret, B.; Enjalbert, M. Data Reconciliation on Multicomponent Network Process. *Comput. Chem. Eng.* **1991**, *17* (8), 807.

(23) Alliet-Gaubert, M.; Joulia, X.; Gerbaud, V.; Mischler, C.; Pons, M.; Serre-Peyrigain, P. *Methodology to Get Process Operating Paths and Multiple Steady States*; AIDIC Symposium Series; AIDIC: Milan, Italy, 2000; Vol. 4.

(24) Renon, H.; Asselineau, L. *Calcul sur Ordinateur des Equilibres Liquide−Vapeur et des Equilibres Liquide−Liquide−Vapeur*; TECHNIP: Paris, France, 1971.

(25) *Prosim, Manuel Utilisateur*; ProSim S.A.: Toulouse, France, 1996 (also see http://www.prosim.fr).

(26) Matsuyama, H.; Nishimura, H. Topological and Thermodynamic Classification of Ternary Vapor−Liquid Equilibrium. *J. Chem. Eng. Jpn.* **1977**, *10*, 181.

(27) Matsuyama, H. Restrictions on Patterns of Residue Curves around Heterogeneous Azeotropes. *J. Chem. Eng. Jpn.* **1978**, *11*, 427.

(28) Benz, S. J.; Scenna, N. J. The Influence of Different Models in Obtaining Multiple Solutions in Distillation Columns. *Can. J. Chem. Eng.* **1997**, *75*, 1142.